

Supplementary Materials for

**Structural basis of X chromosome DNA recognition by the MSL2 CXC
domain during *Drosophila* dosage compensation**

Sanduo Zheng, Raffaella Villa, Jia Wang, Yingang Feng, Jinfeng Wang, Peter B. Becker and Keqiong Ye

Include 6 figures

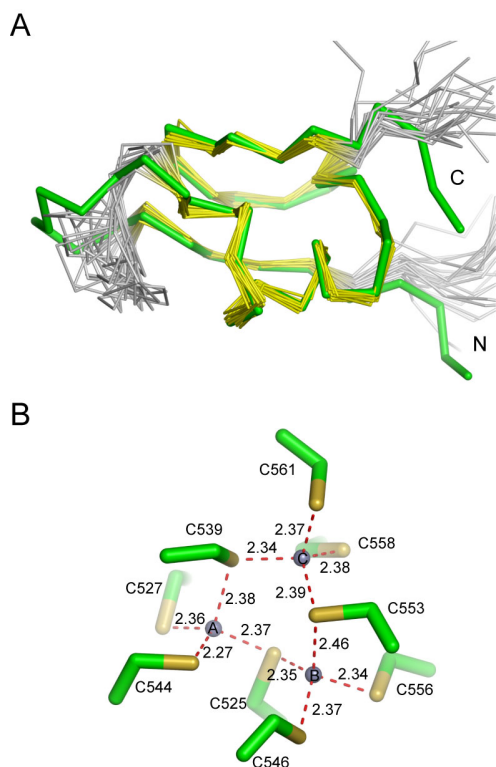


Figure S1. Crystal structure of the CXC domain.

(A) Alignment of the crystal and NMR structure. The 20 NMR structures (PDB code 2LUA) are shown as thin $C\alpha$ traces and colored yellow at the converged core (residues 524-528 and 537-564) and grey at less defined regions. The crystal structure of CXC molecule 2 in the S15 complex is shown as a wide $C\alpha$ trace and colored green. The alignment yields an averaged root mean square deviation of 0.445 Å over 33 $C\alpha$ pairs.

(B) Zn_3Cys_9 cluster in the crystal structure of CXC domain. The length of Zn-S coordination bonds is labeled.

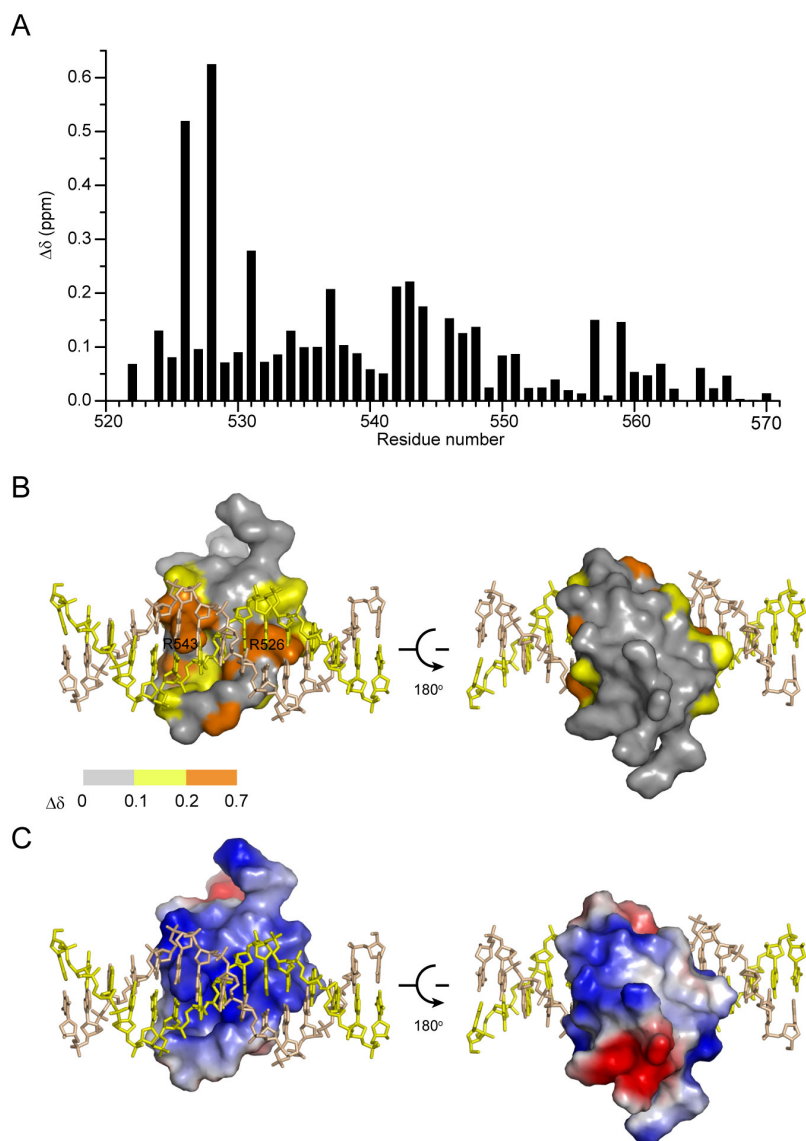


Figure S2. DNA-binding surface of the CXC domain.

(A) The combined chemical shift changes $\Delta\delta$ between the free and S12-bound CXC domain are plotted as a function of residue number. The S12 DNA was present in a 1.5:1 molar ratio to protein.

(B) The DNA-induced chemical shift changes are mapped into the surface of the CXC domain (molecule 2) in the S15 complex structure. Residues are color-coded according to the key. Some significantly perturbed residues are labeled.

(C) Electrostatic potential on the CXC domain. The surface is colored from red to blue for negatively to positively charged regions.

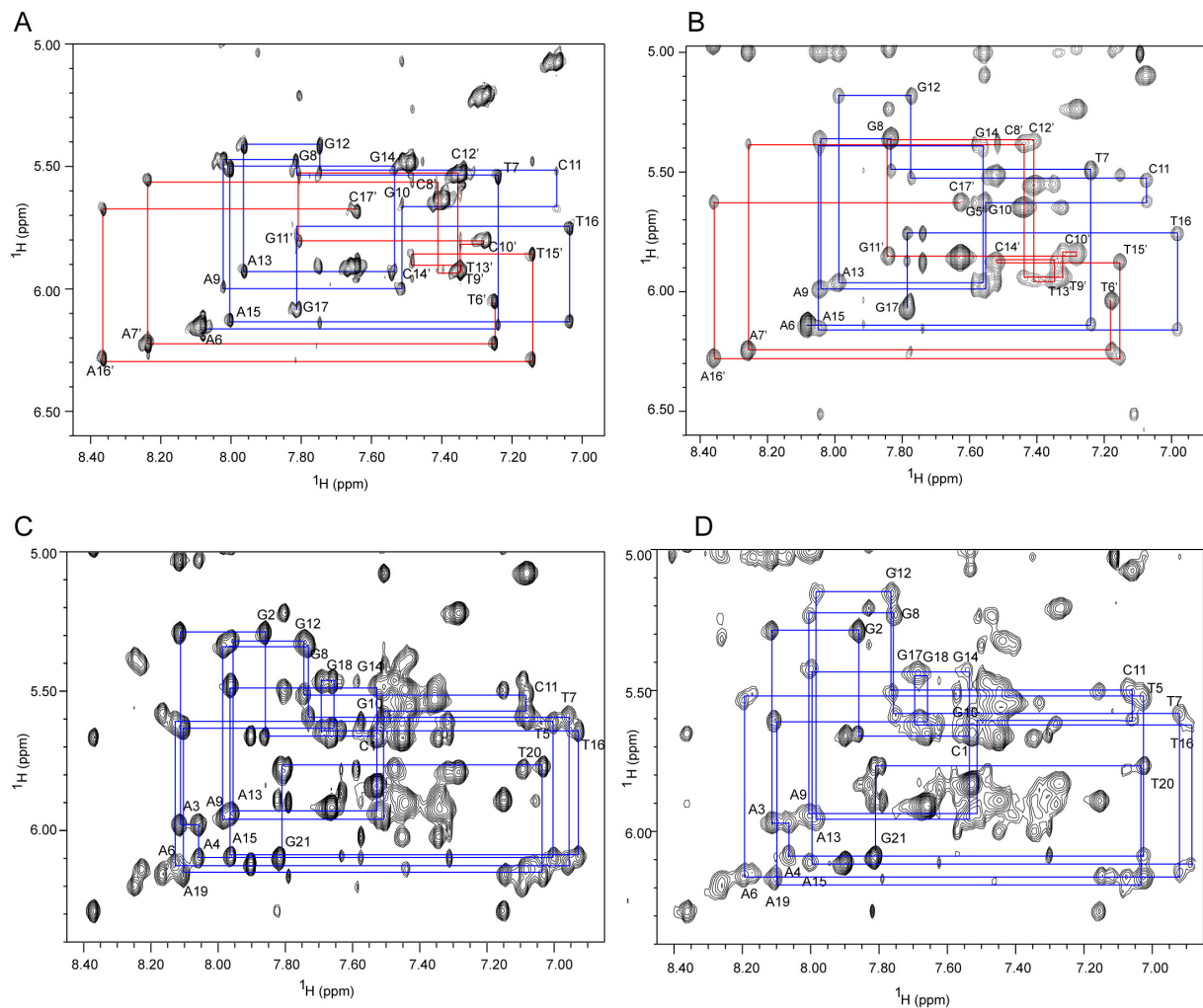


Figure S3. NOESY spectra of MRE DNA and assignments.

(A-D) 2D ^1H - ^1H NOESY spectra of S12 (A, B) and CES11D1 DNA (C, D) in the free state (A, C) and in the presence of one molar equivalent of CXC protein (B, D) at 278 K. The samples contained 1 mM DNA and 0 or 1 mM protein in $^2\text{H}_2\text{O}$ buffer (50 mM phosphate, pH 6.6). The NOE crosspeaks between base H6/8 protons and their own and 5'-flanking sugar H1' protons are connected by blue lines for the top strand and red lines for the bottom strand. The H6/8-H1' crosspeaks from the same nucleotide are labeled.

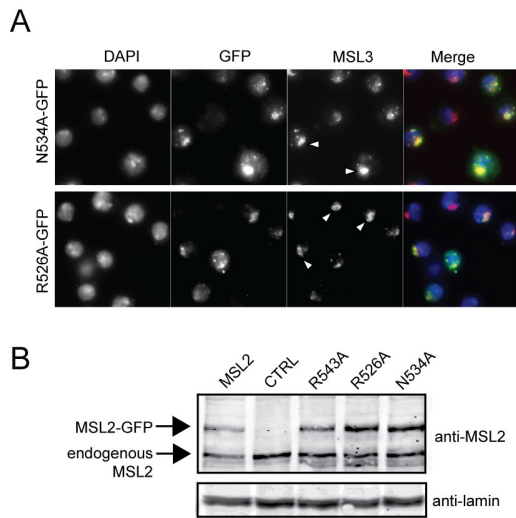


Figure S4. Mutational analysis of CXC domain.

(A) Immunofluorescence analysis of the X-chromosomal territories in S2 cell lines stably expressing MSL2-GFP wt or mutated derivatives (N534A, R526A) using antibodies against GFP and MSL3.

Arrowheads indicate compact, normal X territories. Unmarked GFP-expressing cells lack a distinct chromosomal territory and show delocalized MSL2-GFP and endogenous MSL3.

(B) Western blot analysis of whole cell extracts from S2 cells (CTRL) or S2-derived stable lines expressing MSL2-GFP or MSL2-GFP mutants (R543A, R526A, N534A). The blots were probed with anti-MSL2 and anti-lamin antibodies.

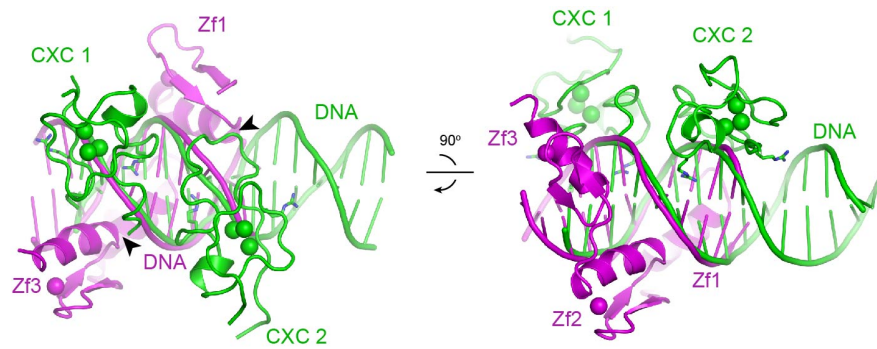


Figure S5. A hypothetical model of the MRE motif bound simultaneously with MSL2 and CLAMP. The DNA complex structure of three Zn-fingers (Zf1-3) of Zif268 (pdb code 1ZAA, magenta) is used as a partial model for the DNA complex of CLAMP that contains 6 consecutive C2H2-type Zn-fingers at the C-terminus. The structure of S15 DNA bound with CXC domains 1 and 2 are colored green. The DNAs from the two structures are aligned to allow minimal clash between the Zn-finger and CXC domains. The arrowheads indicate contact between the Zn-finger and CXC domains at the major groove of DNA. Two orthogonal views are shown.

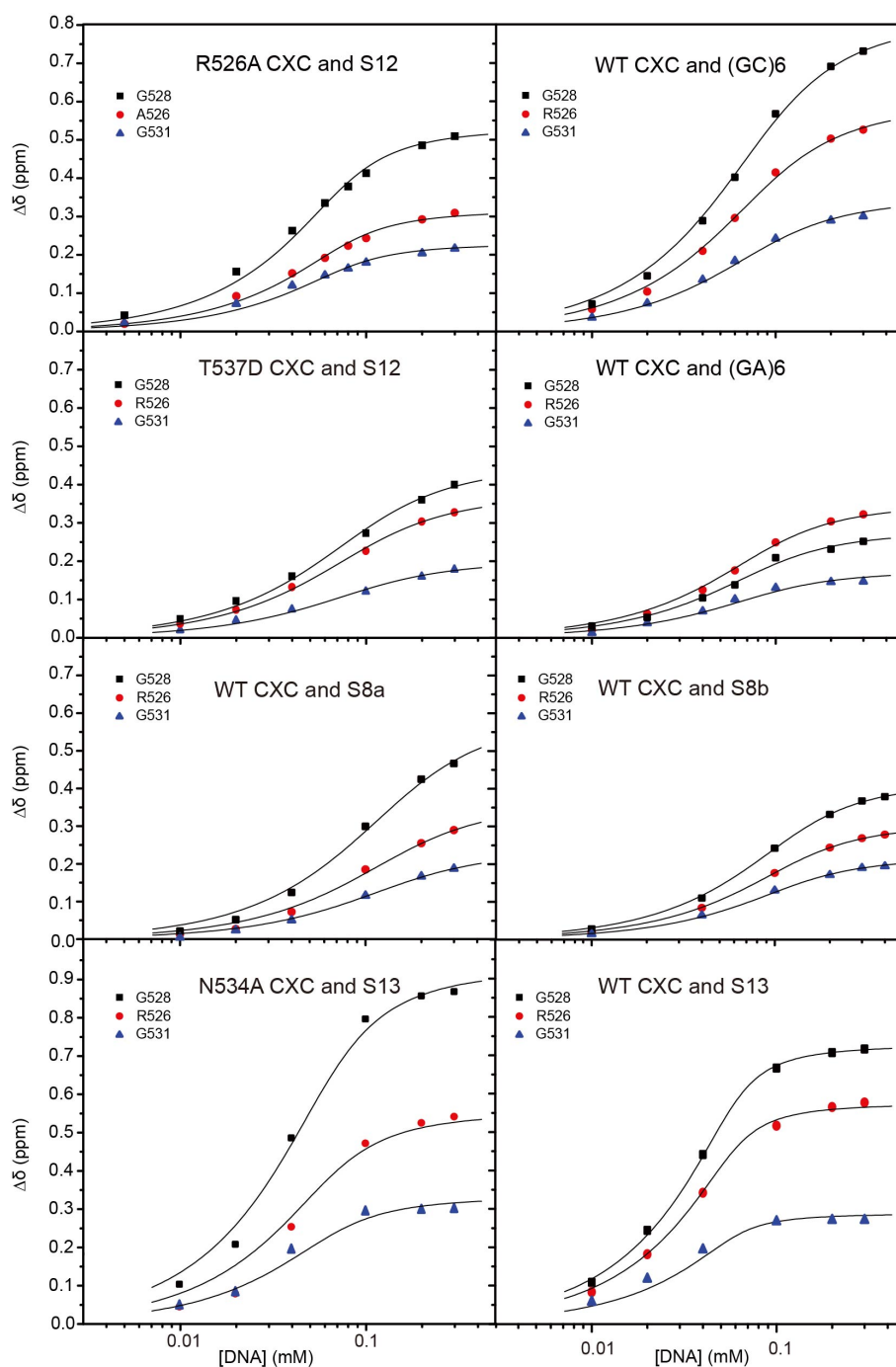


Figure S6. Fitting of DNA titration data of the CXC domain. The WT or mutant CXC domains were titrated with the indicated DNA ligands. The combined chemical shift changes $\Delta\delta$ of three residues (G528, R526 and G531) were globally fit to a binding model described in Materials and Methods. Note that the extent of chemical shift change is sensitive to the particular DNA sequence and the protein mutation. The obtained K_d values are listed in Table 1.